International Journal of Pharmacology

ISSN 1811-7775

science alert

ansinet
Asian Network for Scientific Information

OPEN ACCESS International Journal of Pharmacology

ISSN 1811-7775
DOI: 10.3923/ijp.2025.464.474

Research Article

N-Methylcoclaurine Suppresses Hepatocellular Carcinoma by Inhibiting Protein Disulfide Isomerase *in vitro* and *in vivo*

[1]Yao Fu, [1]Na Zhao, [1]Shihang Zhang, [2]Yue Liu, [1]Changlong Li, [1]Wanting Jiang, [1]Mojiao Zhao and [2,3]Yong Yang

[1]Department of Chinese Medicine and Health Care, Changchun Humanities and Sciences College, Changchun, China
[2]School of Pharmaceutical Sciences, Jilin University, Changchun, China
[3]International College, Krirk University, Bangkok, Thailand

Abstract

Background and Objective: Plumula Nelumbinis (PN) or Lianzixin, is a well-established anti-tumor medicine included by Chinese Pharmacopoeia. Modern pharmacological studies have confirmed that benzylisoquinoline alkaloids are the major anti-tumor components of PN. However, the detailed mechanism remained unclear. This study aimed to evaluate the *in vitro* and *in vivo* anti-tumor effects of *N*-methylcoclaurine (N-MC), a potential natural protein disulfide isomerase (PDI) inhibitor isolated from PN. **Materials and Methods:** Insulin turbidity assay and molecular docking analysis were conducted for the PDI inhibition study of N-MC. The MTT, scratch assay and transwell assays were performed to evaluate the *in vitro* effects of N-MC on HepG2 cells. For the *in vivo* effects of N-MC, the H22-bearing mice model was generated with 40 ICR mice and treated with different doses of N-MC (10, 20 and 40 mg/kg b.wt.). The ANOVA and LSD were performed for the comparisons between groups. **Results:** The N-MC exhibited a concentration-dependent inhibitory effect on PDI, with an IC_{50} of 3.91 μM. The N-MC could fit the active pocket of PDI surrounded by Phe 249, Phe 304, Ile 318, Leu 320, Met 324, Lys 436, Val 437 and His 438, with a calculated binding energy of -8.2 kcal/mol. The N-MC effectively inhibited cell migration and invasion of HepG2 cells in a dose-dependent manner. In the H22 tumor-bearing ICR mice model, N-MC also exhibited dose-dependent tumor suppression quantified by tumor inhibition rates and cell number index. **Conclusion:** The N-MC exhibits the ability to inhibit tumor proliferation, migration and invasion through the inhibition of PDI activity *in vitro* and effectively suppresses tumor growth *in vivo*. These findings suggest that N-MC is a promising candidate for anti-tumor drugs through inhibiting PDI.

Key words: *N*-methylcoclaurine, protein disulfide isomerase, human hepatocellular carcinoma, tumor-bearing mice, anti-tumor

Citation: Fu, Y., N. Zhao, S. Zhang, Y. Liu and C. Li *et al*., 2025. *N*-Methylcoclaurine suppresses hepatocellular carcinoma by inhibiting protein disulfide isomerase *in vitro* and *in vivo*. Int. J. Pharmacol., 21: 464-474.

Corresponding Author: Mojiao Zhao, Department of Chinese Medicine and Health Care, Changchun Humanities and Sciences College, Changchun, China

Copyright: © 2025 Yao Fu *et al*. This is an open access article distributed under the terms of the creative commons attribution License, which permits unrestricted use, distribution and reproduction in any medium, provided the original author and source are credited.

Competing Interest: The authors have declared that no competing interest exists.

Data Availability: All relevant data are within the paper and its supporting information files.

INTRODUCTION

Hepatocellular carcinoma (HCC) is one of the most common malignant tumors worldwide, ranking as the sixth most prevalent cancer and the third leading cause of cancer-related death[1,2]. Traditional Chinese Medicine (TCM) has undergone rigorous clinical validation for its efficacy in treating malignant HCC for thousands of years, offering unique advantages with minimal side effects, multifaceted and multi-target effects at various stages of the disease[3]. According to ClinicalTrials.gov, there are currently 36 registered clinical trials on TCM treatment in HCC[4]. Additionally, extensive *in vivo* and in *vitro* exploration of the mechanisms of TCM in treating HCC has been performed[3,5-8], suggesting that the clinical application of TCM in suppressing HCC is commendable.

Plumula Nelumbinis (PN) or Lianzixin, a renowned TCM included by Chinese Pharmacopoeia, is derived from the dried young leaves and embryonic roots of *Nelumbo nucifera* Gaertn[9]. The major bioactive constituents in PN are alkaloids such as *N*-methylcoclaurine (N-MC), neferine, liensinine and isoliensinine, which belong to benzylisoquinoline subtypes[10]. Modern pharmacology has confirmed the wide range of pharmacological activities and therapeutic value of these benzylisoquinoline alkaloids isolated from PN, including lipid regulation, antioxidant properties, anti-inflammatory effects, antimicrobial actions, blood glucose reduction, anti-depressant effects, anti-fibrotic properties and anti-tumor activities[11-13].

Protein disulfide isomerase (PDI), a versatile thiol oxidoreductase, is recognized as a novel prognostic biomarker and therapeutic target for cancer treatment[14]. Elevated expression of PDI is closely associated with the invasion and metastasis of various tumors, including acute myeloid leukemia, non-small cell lung cancer, melanoma, glioma, prostate and ovarian cancer[14-18]. As an endoplasmic reticulum (ER) chaperone protein, PDI facilitates protein folding and helps tumor cells evade ER stress or the unfolded protein response (UPR) induced cell death. Considering the pivotal role of PDI in the survival and death of UPR-related cell[19], several PDI inhibitors have been identified for various diseases, including ovarian cancer, Huntington's disease, HIV infection, multiple Myeloma, thrombus and glioblastoma[14,20,21]. However, there are currently no clinically approved effective and safe PDI inhibitors.

Previous studies suggested that alkaloids from PN could have an anti-tumor effect. However, the detailed mechanism remained unclear. The N-MC and other alkaloids isolated from PN could inhibit PDI enzyme activity *in vitro*[10]. The present study aimed to verify the PDI inhibitory effect and evaluate the *in vitro* and *in vivo* anti-tumor effects of N-MC.

MATERIALS AND METHODS

Study area: The study was conducted in the Department of Chinese Medicine and Health Care, Changchun Humanities and Sciences College, Changchun, China, from January, 2023 to May, 2024.

Materials and reagents: Plumula Nelumbinis was obtained from Jilin Pharmacy Co., Ltd. (Changchun, China) and authenticated by Professor Zhang Dafang of Changchun Humanities and Sciences College, Changchun, China. A voucher sample (#NP-CC-2023052301) is reserved in the Department of Chinese Medicine and Health Care, Changchun Humanities and Sciences College. The HCC cell lines, HepG2 and H22, were kindly provided by Professor Lijing Li, College of Pharmacy, Changchun University of Chinese Medicine. The PDI siRNA (sc-44319) and control siRNA (sc-44236) were obtained from Univ Biotechnology (Shanghai, China). Dulbecco's Modified Eagle Medium (DMEM, #11995), Roswell Park Memorial Institute 1640 medium (RPMI 1640 medium, #11875093), Penicillin/Streptomycin (#15140) and Lipofectamine 2000 (#11668030) were purchased from Gibco Thermo Fisher. Fetal bovine serum (FBS, #C0226) and Thiazolyl Blue Tetrazolium Bromide (MTT, # ST316) were obtained from Beyotime Biotechnology (Beijing China). Millicell cell culture insert (8 µm, PTEP24H48), Matrigel (E6909), Dithiothreitol (DTT, #43819), insulin (#I4011) and bovine PDI (#P3818) were all purchased from Sigma. *N*-methylcoclaurine was isolated from Plumula Nelumbinis as described by Yang *et al.*[10].

Insulin turbidity assay: The PDI enzyme activity was evaluated using the insulin turbidity assay as described by Zhao *et al.*[22]. Briefly, 1µM PDI was dissolved in 0.1 M KH_2PO_4 and 2 mM EDTA buffer. About 2.5 µL *N*-methylcoclaurine dissolved in Dimethyl Sulfoxide (DMSO) at various concentrations (1, 2, 3, 5 and 10 µM, respectively) was incubated with 1 µM PDI for 1 hr at 37°C. Subsequently, 20 µL of 0.65 mM insulin dissolved in 5 mM HCl, 2.5 mM DTT, 0.1 M KH_2PO_4 and 2 mM EDTA buffer, was added to the mixture solution. Absorbance values at 620 nm were recorded every 2 min for 80 min using a microplate reader (Bio-Rad Laboratories, Hercules, California, USA). The negative control (insulin only) group, which did not contain PDI represented 100% inhibition (0% activity). The positive control group (without inhibitors added) contains PDI and insulin, exerting 100% activity or 0% inhibition of PDI enzymatic activity, PDI activity (%) = OD_{620} (test groups-negative control)/OD_{620} (positive control-negative control)×100%. Nonlinear regression analysis was performed to calculate IC_{50} values.

Molecular docking: The crystal structure of the human PDI bb'a' domains co-crystallization with (4s, 5s)-1,2-dithiane -4,5-diol (PDB entry code: 3UEM) was downloaded from RCSB PDB with a resolution of 2.29 Å[23]. Molecular docking was performed using Discovery Studio 4.5 (BIOVIA, San Diego, California, USA) and CDOCKER protocol to dock *N*-methylcoclaurine into 3UEM. Before docking, all water molecules were removed and hydrogen atoms were added to the 3UEM structure as described by Zhao *et al.*[22].

Cell culture and siRNA transfection: The HepG2 cells were cultured in DMEM supplemented with 1% penicillin/ streptomycin and 10% FBS at 37°C. The siRNA powder was suspended in 66 µL of RNase-free water to achieve a 10 µM siRNA stock solution. The HepG2 cells (500 µL) were treated with 20 pmol PDI siRNA or control siRNA (40 nM) and 1 µL Lipofectamine 2000 in 24 wells plates. The mRNA expression level of PDI was verified by real time-PCR 48 hrs after transfection. Cells were stained with 0.2% crystal violet and cell numbers were analyzed using ImageJ (Version 1.54k 15). The cell number index used for quantifying stained cells was calculated as the ratio of the cell number in the test group to the cell number in the siCtl group.

Cell viability analysis by MTT assay: The cell viability of HepG2 cells was assessed using the MTT proliferation assay[22]. After 24 hrs of culture of HepG2 cells at 37°C, cells seeded in 96 well plates were treated with different concentrations of the N-MC for another 24 hrs. Removed the culture medium and washed the cells with PBS three times. The 20 µL MTT solution (5 mg/mL) was added to each well and incubated at 37°C for 4 hrs. The supernatant was aspirated, 50 µL of DMSO was added and the plates were shaken for 10 minutes to dissolve the purple formazan crystals. Absorbance at 490 nm was measured using a microplate reader (Bio-Rad Laboratories, Hercules, California, USA). Cell viability percentages were calculated by dividing the OD_{490} of the test group by that of the control group.

Cell migration assay: The cell migration was assessed using the *in vitro* scratch assay[24]. The HepG2 cells were plated onto the 12-well plates to create a confluent monolayer. Artificial gaps were created by p200 pipette tips. The plates were washed with PBS and growth medium sequentially to remove the floating cells and debris. Cells were incubated in a medium containing DMSO or indicated concentration of N-MC. Images were taken with an Osteoplan II microscope (Carl Zeiss, NY) at, 24 and 48 hrs after the scratch was made. Migration rates (gap areas of 24 or 48 hrs normalized by 0h group) were analyzed using ImageJ developed by NIH[25].

Cell invasion assay: The cell invasion capability was assessed using transwell *in vitro* cell invasion assays[26]. Extracellular matrix (ECM) coating process followed the protocol provided by Sigma. The HepG2 cells were pretreated with indicated concentrations of *N*-methylcoclaurine for 24 hrs in 24 well plates. Cells (100 mL) suspended in medium without FBS were transferred into Millicell cell culture inserts and 600 µL culture medium with 10% FBS was placed in the bottom chamber. Non-invasive cells on the apical side of the insert membrane were gently removed with sterile cotton tips. The bottom side of the inserts was fixed in 70% ethanol and stained with 0.2% crystal violet.

Animals and experiment procedure: The ICR mice (6 weeks old, 18-22 g, License No. SCXK (Jing) 2009-0004) used in this study were all obtained from the Animal Center of Changchun Humanities and Sciences College and maintained under SPF standards at 22±3°C with 12 hrs light/dark cycle. A standard diet and water were provided throughout the experiment. All experimental procedures carried out followed the Guidelines for Animal Experiments and were approved by the Institutional Ethics Committee of Changchun Humanities and Sciences College (Approval No. CCHSC-20220926005). Forty mice were evenly randomized and divided into 5 groups with 8 mice each, H22 malignant ascites culture group (2 for 1st ascites, 2 for 2nd ascites and 4 for 3rd ascites), H22 model group, low dose group (10 mg/kg b.wt., N-MC), medium dose group (20 mg/kg b.wt., N-MC) and high dose group (40 mg/kg b.wt., N-MC). The H22 cells were cultured in 1640 medium containing 10% FBS and 1% penicillin and streptomycin at 37°C 200 µL. After three generations of malignant ascites culture, H22 cell suspension in pre-cooled PBS (1:4, 5×10^6/mL) or PBS alone (normal group) was subcutaneously injected into the armpits of the animals. The N-MC treated groups were continuously administered different concentrations of N-MC solution intragastrically for 2 weeks. The normal group and H22 model group were administrated saline instead. The 24 hrs after the last dosing, all mice were anesthetized with CO_2. All the tumor tissues from each animal were obtained and weighed[27]:

$$\text{Tumor inhibition rate (\%)} = \frac{\text{1-treatment group mean tumor weight}}{\text{Saline group mean tumor weight}} \times 100$$

Detached the tumor and cut into 1×1×0.3 cm blocks. Fixed in paraformaldehyde for 48 hrs and embedded in paraffin. The remaining tissues were stored at -80°C until further assessment. Observe the pathological changes of tumor tissue in each group under an Osteoplan II microscope (Carl Zeiss and NY) after H&E staining.

Statistical analysis: Data analysis was performed using the SPSS 25.0 package (SPSS Inc, Chicago, IL). Data were shown as Means±SD of more than triple replicates. Nonlinear regression analysis provided by SPSS was performed to calculate IC_{50} and CC_{50} values. The ANOVA and LSD were performed for the comparisons between the two groups. Significance was set at $p<0.05$.

RESULTS

***N*-methylcoclaurine inhibits PDI activity by insulin turbidity assay:** To investigate whether *N*-methylcoclaurine (N-MC, Fig. 1a) exerts inhibitory effects on PDI enzymatic activity, insulin turbidity assays with varying concentrations of N-MC were performed, including 1, 2, 3, 5 and 10 μM. As illustrated in Fig. 1b, the blank group (absence of N-MC) exhibited the highest absorbance at 620 nm (left Y-axis), with a theoretical inhibition rate of 0% (right Y-axis). Conversely, the positive control group (without PDI) displayed the lowest absorbance at 620 nm and a 100% inhibition rate. According to the formula described in "insulin turbidity assay" section, the inhibition rates of N-MC at concentrations of 1, 2, 3, 5 and 10 μM on PDI activity were determined as 15.01, 23.21, 30.05, 71.89 and 85.35%, respectively, indicating a concentration-dependent inhibitory effect on PDI. As shown in Fig. 1c, the IC_{50} of N-MC in PDI inhibition is 3.91 μM.

***N*-methylcoclaurine fits the active pocket of PDI by molecular docking:** To further confirm the interaction between N-MC and PDI, molecular docking was performed using the crystal structure of the human PDI bb'a' domain (PDB entry: 3UEM) obtained from the PDB database. The co-crystallized binding site of (4S,5S)-1,2-dithiane-4,5-diol with PDI served as the central docking region and the molecular docking of PDI with N-MC was conducted using Discovery Studio 4.5 software and Autodock Vina. As depicted in Fig. 1d, N-MC is surrounded by Phe 249, Phe 304, Ile 318, Leu 320, Met 324, Lys 436, Val 437 and His 438 of 3UEM. The calculated binding energy between N-MC and 3UEM using Autodock Vina was -8.2 kcal/mol. Notably, Phe 249 and Lys 436 form hydrogen bonds with 3UEM. This docking analysis provides evidence of the specific interaction between N-MC and the PDI binding site, further supporting the potential inhibitory effect of N-MC on PDI function.

Effects of *N*-methylcoclaurine on cell viability of HepG2 cells: To examine the morphological changes in HepG2 cells caused by N-MC, crystal violet staining was performed after 24 hrs of treatment with different concentrations of N-MC (1 and 10 μM), using siPDI as a positive control (Fig. 2a). To verify the effect of siPDI on mRNA levels of PDI, real-time PCR was conducted. Compared to the control siRNA (siCtl) treated group, an average reduction of 21.0% was detected after siPDI treatment (Fig. 2b). To quantify the cell number after staining, the cell number index normalized to the siCtl (Fig. 2c). The siPDI transfected group significantly reduced the cell number index to 0.21 ($p<0.01$), suggesting that PDI inhibition suppresses the viability of HepG2 cells. Compared to the control, N-MC significantly reduced the cell number index to 0.76 and 0.22 when treated with 1 and 10 μM N-MC, respectively. To investigate the effects of N-MC on HepG2 viability, we performed an MTT assay using different concentrations of N-MC, including 1, 5 and 10 μM (Fig. 2d). Compared to the control group, N-MC showed significant suppression effects on HepG2 proliferation, with survival rates of 79.46, 60.32 and 17.06 for 1, 3 and 10 μM N-MC, respectively. As shown in (Fig. 2e), the CC_{50} of N-MC is 5.44 μM.

Effects of *N*-methylcoclaurine on cell migration and invasion of HepG2 cells: To investigate the effects of N-MC on the migration of HepG2 cells, *in vitro* scratch assays with varying concentrations of N-MC were conducted, including 1, 5 and 10 μM (Fig. 3a). According to the migration rates formula described in "cell migration assay" section, the migration rates of the control group were 65.15 and 86.93% at 24 and 48 hrs, respectively. In comparison, the migration rates in the low-dose, medium-dose and high-dose groups after 24 and 48 hrs of treatment, were 47.76, 42.02 and 34.45%, as well as 53.97, 46.57 and 35.96%, respectively, showing significant reductions compared to the control group (all $p<0.05$) (Fig. 3b). Results were consistent after further validation by crystal violet staining at 48 hrs (Fig. 3c). To assess the impact of low, medium and high concentrations (1, 5 and 10 μM) of N-MC on HepG2 cell invasion, transwell *in vitro* cell invasion assays were conducted (Fig. 4a). The results in (Fig. 4b) demonstrated that N-MC effectively inhibited HepG2 cell invasion at all three concentrations, showing a concentration-dependent response ($p<0.05$).

Effects of *N*-methylcoclaurine on tumor suppression in H22-bearing mice: To further investigate the *in vivo* effects of N-MC on hepatocellular carcinoma, a tumor-bearing ICR mouse model by subcutaneously injecting 3rd generation of H22 ascites into the armpits of the animals was generated (Fig. 5a). To evaluate the potentially

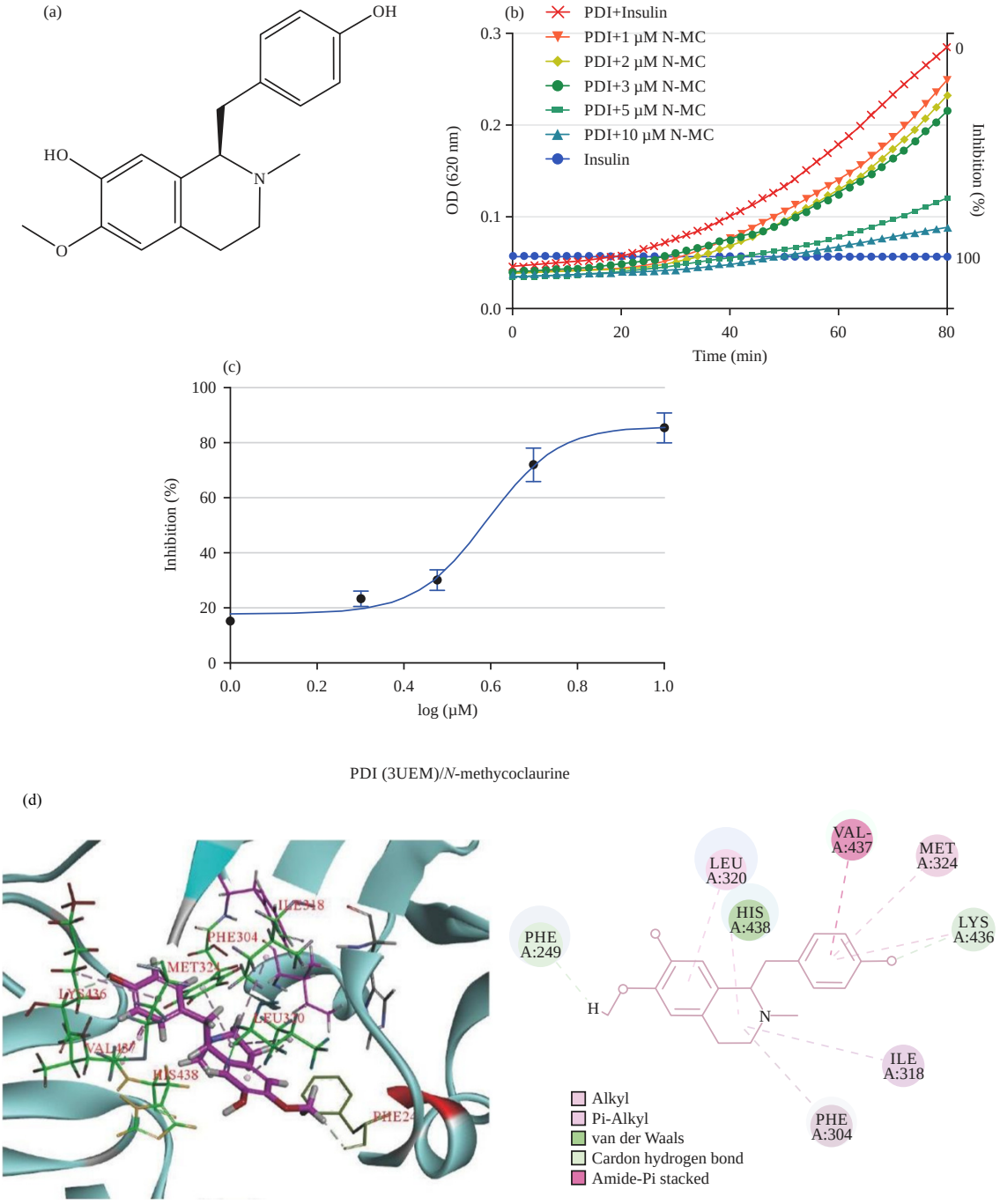

Fig. 1(a-d): Inhibitory effects of *N*-methylcoclaurine on PDI *in vitro* and *in silico*, (a) Chemical structure of *N*-methylcoclaurine (N-MC), (b) Absorption curves at 620 nm of insulin turbidity assay using different concentrations of N-MC, (c) Inhibition curve of N-MC on PDI enzyme activity. The dashed line indicates the IC_{50} value and (d) 3D and 2D predicted docking patens of N-MC into PDI (PDB #3UEM)

N-MC: *N*-methylcoclaurine and PDI: Protein disulfide isomerase

harmful effects of N-MC in mice, body weights were recorded every 2 days and no significant changes were observed during the experimental process (Fig. 5b). Morphological images of representative tumors dissected from animals in each group are shown in (Fig. 5c). Compared to the saline group, the N-MC-treated groups exhibited reductions in tumor size. To quantify the tumor size reduction, tumor inhibition rates were calculated

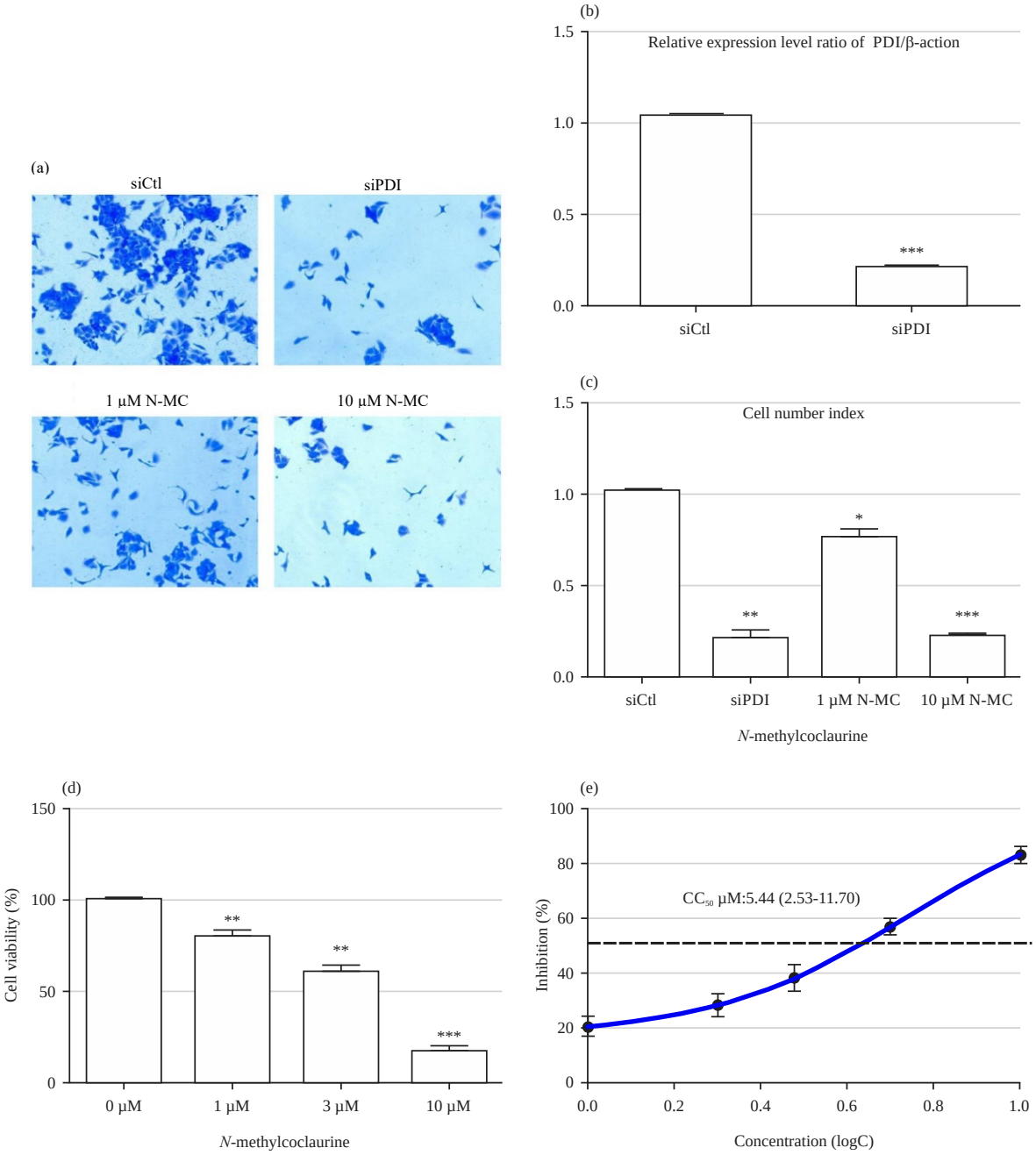

Fig. 2(a-e): Effects of *N*-methylcoclaurine on viability of HepG2 cell, (a) Crystal violet staining, (b) Quantitative calculation indicated by cell number index, (c) Relative mRNA expression level of PDI, (d) Results of MTT assays and (e) CC_{50} curves were generated from mean values of inhibition (%) treated by N-MC of 1, 2, 3, 5 and 10 µM for 48 hrs

siCtl: Treatment by control siRNA, siPDI: Groups treated by PDI siRNA. *, **, ***p< 0.05, 0.01 and 0.005 of comparison between test group and control group shown in (E), MTT: 3-(4,5-dimethylthiazol-2-yl)-2,5-diphenyltetrazolium bromide and CC_{50}: 50% cytotoxic concentration

(as described in the "animals and experiment procedure" section). As shown in Fig. 5d, compared to the saline group, N-MC at 10, 20 and 40 mg/kg/day notably and dose-dependently inhibited tumor growth by 42.27, 54.63 and 63.67%, respectively.

To examine the inner structural changes of the tumor-induced by N-MC, Hematoxylin and Eosin (H&E) staining were performed. In the saline group, the tumor cells were evenly distributed and no obvious vacuoles were observed (Fig. 5e). Compared to the saline group, the N-MC-treated

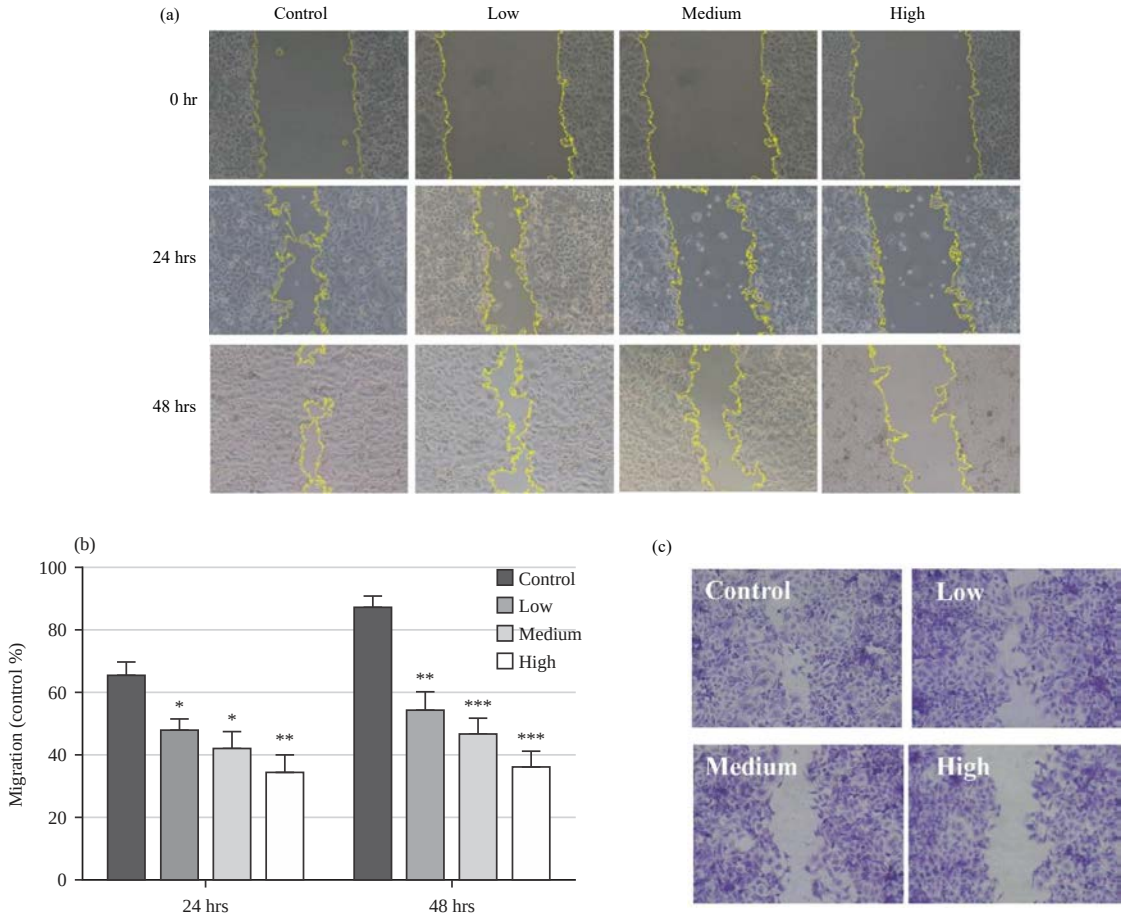

Fig. 3(a-c): Inhibitory effects of *N*-methylcoclaurine on cell migration of HepG2 by *in vitro* scratch assay, (a) Progressive changes of the scratched wound were imaged at 0, 24 and 48 hrs, (b) Cell migration rate and (c) Morphology of cells around the wound

Control: DMSO treated group, Low: Low concentration (1 μM) of N-MC, Medium: Medium concentration (3 μM) of N-MC and High: High concentration (10 μM) of N-MC

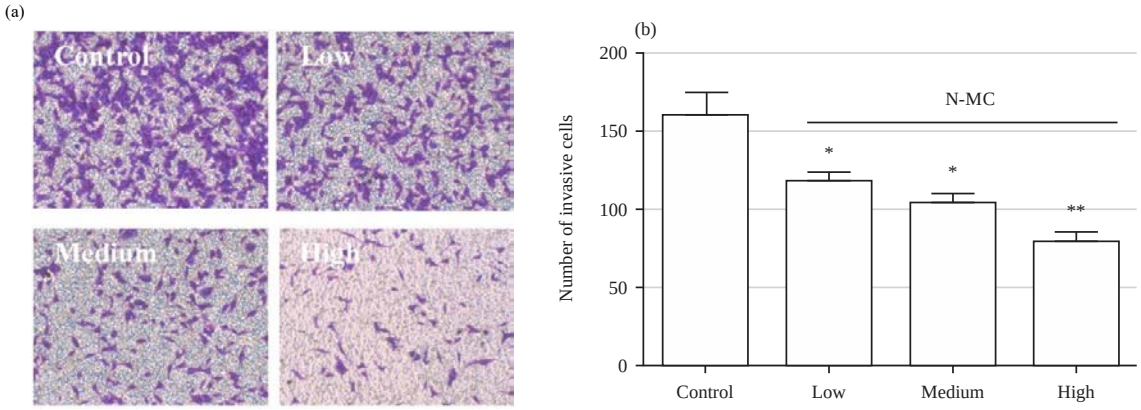

Fig. 4(a-b): Inhibitory effects of *N*-methylcoclaurine on cell invasion of HepG2 by transwell *in vitro* cell invasion assays

HepG2 cells were pre-treated with low concentration (1 μM), medium concentration (3 μM) and high concentration (10 μM) of N-MC for 24 hrs, (a) Representative images after 0.2% crystal violet staining and (b) Quantification of invasive HepG2 cells Values are shown as Mean±SD of triplicate experiments, *p<0.05 and **p<0.01, versus control groups

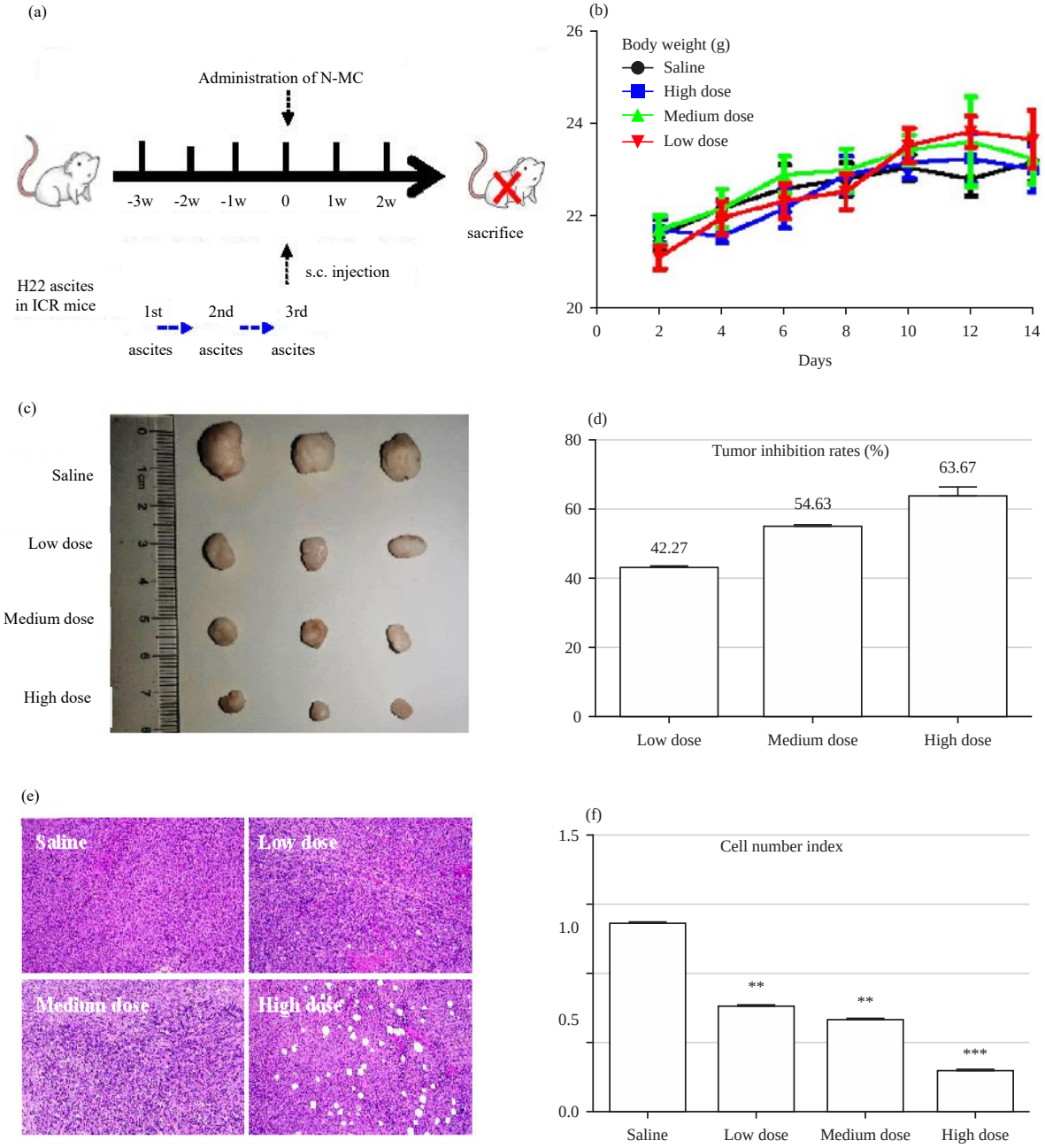

Fig. 5(a-e): Effects of *N*-methylcoclaurine on H22 tumor-bearing ICR mice, (a) Schematic procedure of the animal experiment, (b) Body weights recorded every 2 days, (c) Tumor images of each group, (d) Tumor inhibition rates, (e) H&E staining images and (f) Cell number index

Values are expressed as Mean±SD of triplicate experiments, **p<0.01, ***p<0.005 and versus control groups

group exhibited various degrees of cell loss and white vacuoles. To quantify the tumor cell loss, the cell number index was calculated (as described in the "cell culture and siRNA transfection" section). Compared to the saline group, the remaining cell number indicated by the cell number index in the N-MC treated group all decreased significantly (all p<0.05, Fig. 5f).

DISCUSSION

The present study verified the PDI inhibitory effects of N-MC and evaluated anti-tumor effects in the human Hepatocellular Carcinoma Cell Line (HepG2) and tumor-bearing mice model (H22). Interaction between PDI and N-MC was first validated using two independent assays *in vitro*

and *in silico*. The insulin turbidity *in vitro* assay is a well-established method for measuring PDI activity based on the stability of the insulin B chain. The PDI-mediated breakage of disulfide bonds between chains A and B leads to the aggregation of the B chain, resulting in increased absorption around 620 nm[1]. In the present study, the inhibitory effects of N-MC on PDI are found to be concentration-dependent, with an IC_{50} of 3.91 μM. To investigate the possible physical interaction between PDI and N-MC, we performed molecular docking *in silico* analysis based on the crystal structure of the human PDI bb'a' domain (PDB #3UEM) as previously described by Singal *et al.*[2]. The docking analysis indicated that N-MC is surrounded by residues Phe 249, Phe 304, Ile 318, Leu 320, Met 324, Lys 436, Val 437 and His 438, with a binding energy of -8.2 kcal/mol, reinforcing the potential influence of N-MC on PDI function. Considering the results of insulin turbidity assay and molecular docking analysis, N-MC derived from Plumula Nelumbinis (PN) was suggested as a promising PDI inhibitor.

To investigate the effects of N-MC on HCC, cell viability, invasion and migration in the HepG2 cell line *in vitro* and in an H22 tumor-bearing mice model *in vivo* were examined. Consistent with the tumor suppression effects of PDI inhibition in other types of tumors, an 80% reduction in cell viability in the HepG2 cell line by PDI siRNA. Additionally, N-MC exhibited cytostatic capacity in HepG2 cells with a CC_{50} (50% cytotoxic concentration) of 5.44 μM (Fig. 2c). Given the correlation of PDI upregulation with cancer metastasis and invasion in other cancer types, cell invasion and migration in HepG2 cells were also examined using transwell and scratch assay, respectively. The results shown in Fig. 3 and 4 demonstrated that N-MC effectively inhibited HepG2 cell migration and invasion at all three concentrations in a concentration-dependent manner ($p<0.05$). *In vivo* studies further demonstrated that N-MC significantly and dose-dependently suppressed tumor growth in H22 tumor-bearing mice, with inhibition rates of 42.27, 54.63 and 63.67% at doses of 10, 20 and 40 mg/kg/day, respectively. Hematoxylin and Eosin (H&E) staining indicated substantial changes in the internal structure of tumors in the N-MC-treated group compared to the saline group, with varying degrees of cell loss and white vacuoles evident.

Plumula Nelumbinis (PN) also known as lotus seeds or Lianzixin, have been used as a traditional Chinese medicine for thousands of years and are considered valuable for tumor treatment[28]. Consistent with its traditional use, studies from other groups have shown that ethanol extract of *Nelumbo nucifera* stamen[29], total alkaloids from Ba lotus seed[30] and individual benzylisoquinoline alkaloids isolated from PN, such as neferine[31] and liensinine[32] exhibit significant anti-tumor effects. The PDI is an ER-localized chaperone overexpressed in various types of cancers, including acute myeloid leukemia, multiple myeloma, breast cancer, ovarian cancer, lung cancer, glioma, melanoma and prostate cancer. Elevated expression of PDI was found to benefit tumor growth, metastasis and invasion. Therefore, PDI inhibition has recently been considered a promising therapeutic strategy against tumors by increasing protein misfolding-related cell death or ER stress. However, whether the alkaloids isolated from PN could inhibit PDI remained unclear.

Despite several PDI inhibitors being identified from natural products or chemical synthesis, there are still no clinically approved safe and effective agents. Therefore, developing PDI inhibitors for clinical purposes remains important. Previously, N-MC isolated from PN was reported to inhibit PDI *in vitro*[3]. In this study, the suppression effects of N-MC against HCC *in vitro* and *in vivo* were further investigated. This compelling evidence suggests N-MC is a promising anti-tumor drug as PDI inhibitors. However, there remained unsolved questions including drug stability study, drug dose form study and clinical pharmacy study (absorption, metabolism and distribution).

CONCLUSION

This study has provided novel insights into the anti-tumor effects of N-MC against HCC *in vitro* and *in vivo*. The findings indicate that N-MC can effectively inhibit PDI enzymatic activity, resulting in suppression of proliferation, migration and invasion of HCC cells, as evidenced by MTT, scratch and transwell assays in HepG2. Moreover, results of H22-bearing mice also support N-MC as a potential drug in HCC treatment. In conclusion, these findings provide future recommendations for developing PDI inhibitors into clinically approved drugs in the treatment of HCC.

SIGNIFICANCE STATEMENT

This study provided a novel insight into the anti-tumor effects of *N*-methylcoclaurine (N-MC) by inhibiting protein disulfide isomerase (PDI) in mice, suggesting promising effective natural PDI inhibitors derived from Plumula Nelumbinis (PN). The results demonstrated that N-MC exhibited concentration-dependent inhibitory effect on PDI *in vitro*. Meanwhile, the *in silico* molecular docking analysis verified N-MC and PDI's interaction. Additionally, this study evaluated the anti-tumor effects of N-MC

both in the human Hepatocellular Carcinoma Cell Line (HepG2) and tumor-bearing mice model (H22). Collectively, the findings contribute to novel insights into anti-tumor strategies targeting PDI and provide future recommendations for developing N-MC into clinically effective drugs in the treatment of hepatocellular carcinoma.

REFERENCES

1. Llovet, J.M., R.K. Kelley, A. Villanueva, A.G. Singal and E. Pikarsky *et al*., 2021. Hepatocellular carcinoma. Nat. Rev. Dis. Primers, Vol. 7. 10.1038/s41572-020-00240-3.
2. Singal, A.G., F. Kanwal and J.M. Llovet, 2023. Global trends in hepatocellular carcinoma epidemiology: Implications for screening, prevention and therapy. Nat. Rev. Clin. Oncol., 20: 864-884.
3. Liu, C., S. Yang, K. Wang, X. Bao and Y. Liu *et al*., 2019. Alkaloids from traditional Chinese medicine against hepatocellular carcinoma. Biomed. Pharmacother., Vol. 120. 10.1016/j.biopha.2019.109543.
4. Wu, J., G. Tang, C.S. Cheng, R. Yeerken and Y.T. Chan *et al*., 2024. Traditional Chinese medicine for the treatment of cancers of hepatobiliary system: From clinical evidence to drug discovery. Mol. Cancer, Vol. 23. 10.1186/s12943-024-02136-2.
5. Liu, X., M. Li, X. Wang, Z. Dang and L. Yu *et al*., 2019. Effects of adjuvant traditional Chinese medicine therapy on long-term survival in patients with hepatocellular carcinoma. Phytomedicine, Vol. 62. 10.1016/j.phymed.2019.152930.
6. Zhang, Y., H.G. Chen, C. Zhao, X.J. Gong and X. Zhou, 2020. Research progress on anti-hepatocellular carcinoma mechanism of active ingredients of traditional Chinese medicine. China J. Chin. Materia Med., 45: 3395-3406.
7. Wei, L., Z. Wang, N. Jing, Y. Lu and J. Yang *et al*., 2022. Frontier progress of the combination of modern medicine and traditional Chinese medicine in the treatment of hepatocellular carcinoma. Chin. Med., Vol. 17. 10.1186/s13020-022-00645-0.
8. Luo, R., C. Fang, C. Chen, Y. Zhang and R. Yao *et al*., 2023. Adjuvant therapy with Jianpi Huayu decoction improves overall and recurrence-free survival after hepatectomy for hepatocellular carcinoma: A retrospective propensity score-matching study. Front. Pharmacol., Vol. 14. 10.3389/fphar.2023.1212116.
9. Chen, S., X. Li, J. Wu, J. Li and M. Xiao *et al*., 2021. Plumula Nelumbinis: A review of traditional uses, phytochemistry, pharmacology, pharmacokinetics and safety. J. Ethnopharmacol., Vol. 266. 10.1016/j.jep.2020.113429.
10. Yang, Y., X.Z. Li, Q.H. Zhang and D. Lu, 2017. Studies on the chemical components of Nelumbinis Plumula and the inhibitory activity on protein disulfide isomerase. China J. Chin. Materia Med., 42: 3004-3010.
11. Rajput, M.A. and R.A. Khan, 2017. Phytochemical screening, acute toxicity, anxiolytic and antidepressant activities of the *Nelumbo nucifera* fruit. Metab. Brain Dis., 32: 743-749.
12. Zheng, Q., J. Chen, Y. Yuan, X. Zhang and L. Li *et al*., 2022. Structural characterization, antioxidant, and anti-inflammatory activity of polysaccharides from Plumula Nelumbinis. Int. J. Biol. Macromol., 212: 111-122.
13. Wang, X., Z. Wei, P. Hu, W. Xia and Z. Liao *et al*., 2023. Optimization of neferine purification based on response surface methodology and its anti-metastasis mechanism on HepG2 cells. Molecules, Vol. 28. 10.3390/molecules28135086.
14. Xu, S., S. Sankar and N. Neamati, 2014. Protein disulfide isomerase: A promising target for cancer therapy. Drug Discovery Today, 19: 222-240.
15. Yang, S., C. Jackson, E. Karapetyan, P. Dutta and D. Kermah *et al*., 2022. Roles of protein disulfide isomerase in breast cancer. Cancers, Vol. 14. 10.3390/cancers14030745.
16. Paglia, G., M. Minacori, G. Meschiari, S. Fiorini, S. Chichiarelli, M. Eufemi and F. Altieri, 2023. Protein disulfide isomerase A3 (PDIA3): A pharmacological target in glioblastoma? Int. J. Mol. Sci., Vol. 24. 10.3390/ijms241713279.
17. Smulders-Srinivasan, T.K., S.E. Jenkinson, L.J. Brown, V.P. Lenis and R. Bass, 2023. *PDIA6* and *Maspin* in prostate cancer. Anticancer Res., 43: 5331-5340.
18. Ichiki, N., C. Saigo, Y. Hanamatsu, H. Iwata and T. Takeuchi, 2024. Inducing melanoma cell apoptosis by ERp57/PDIA3 antibody in the presence of CPI-613 and hydroxychloroquine. J. Cancer, 15: 1779-1785.
19. Zhang, Z., L. Zhang, L. Zhou, Y. Lei, Y. Zhang and C. Huang, 2019. Redox signaling and unfolded protein response coordinate cell fate decisions under ER stress. Redox Biol., Vol. 25. 10.1016/j.redox.2018.11.005.
20. Wang, B., J. Zhang, X. Liu, Q. Chai and X. Lu *et al*., 2022. Protein disulfide isomerases (PDIs) negatively regulate ebolavirus structural glycoprotein expression in the endoplasmic reticulum (ER) via the autophagy-lysosomal pathway. Autophagy, 18: 2350-2367.
21. Wang, N.C., H.W. Chen and T.Y. Lin, 2023. Association of protein disulfide isomerase family A, member 4, and inflammation in people living with HIV. Int. J. Infect. Dis., 126: 79-86.
22. Zhao, M., C. Zhang, D. Zhang, S. Zhu and T. Liu *et al*., 2021. Dicentrine and dicentrinone isolated from *Stephania tetrandrae* radix suppress HepG2 proliferation through inhibiting PDI activity. Rec. Nat. Prod., 15: 396-407.
23. Wang, C., J. Yu, L. Huo, L. Wang, W. Feng and C.C. Wang, 2012. Human protein-disulfide isomerase is a redox-regulated chaperone activated by oxidation of domain a'. J. Biol. Chem., 287: 1139-1149.
24. Liang, C.C., A.Y. Park and J.L. Guan, 2007. *In vitro* scratch assay: A convenient and inexpensive method for analysis of cell migration *in vitro*. Nat. Protoc., 2: 329-333.

25. Suarez-Arnedo, A., F.T. Figueroa, C. Clavijo, P. Arbeláez, J.C. Cruz and C. Muñoz-Camargo, 2020. An image J plugin for the high throughput image analysis of *in vitro* scratch wound healing assays. PLoS ONE, Vol. 15. 10.1371/journal.pone.0232565.
26. Justus, C.R., M.A. Marie, E.J. Sanderlin and L.V. Yang, 2023. Transwell *in vitro* Cell Migration and Invasion Assays. In: Cell Viability Assays: Methods and Protocols, Friedrich, O. and D.F. Gilbert (Eds.), Humana, New York, ISBN: 978-1-0716-3052-5, pp: 349-359.
27. Lu, Y., S. Zhang, X. Zhu, K. Wang and Y. He *et al*., 2023. Aidi injection enhances the anti-tumor impact of doxorubicin in H22 tumor-containing mice. J. Ethnopharmacol., Vol. 303. 10.1016/j.jep.2022.115968.
28. Arooj, M., S. Imran, M. Inam-ur-Raheem, M.S.R. Rajoka and A. Sameen *et al*., 2021. Lotus seeds (*Nelumbinis semen*) as an emerging therapeutic seed: A comprehensive review. Food Sci. Nutr., 9: 3971-3987.
29. Zhao, X., X. Feng, C. Wang, D. Peng, K. Zhu and J.L. Song, 2017. Anticancer activity of *Nelumbo nucifera* stamen extract in human colon cancer HCT-116 cells *in vitro*. Oncol. Lett., 13: 1470-1478.
30. Zhao, X., X. Feng, D. Peng, W. Liu and P. Sun *et al*., 2016. Anticancer activities of alkaloids extracted from the *Ba lotus* seed in human nasopharyngeal carcinoma CNE-1 cells. Exp. Ther. Med., 12: 3113-3120.
31. Yoon, J.S., H.M. Kim, A.K. Yadunandam, N.H. Kim and H.A. Jung *et al*., 2013. Neferine isolated from *Nelumbo nucifera* enhances anti-cancer activities in Hep3B cells: Molecular mechanisms of cell cycle arrest, ER stress induced apoptosis and anti-angiogenic response. Phytomedicine, 20: 1013-1022.
32. Chang, M., S. Ding, X. Dong, X. Shang and Y. Li *et al*., 2022. Liensinine inhibits cell growth and blocks autophagic flux in nonsmall-cell lung cancer. J. Oncol., Vol. 2022. 10.1155/2022/1533779.